

Reduced Transport Models for a Tokamak Flight Simulator

M. Muraca¹, E. Fable¹, C. Angioni¹, P. David¹, T. Luda¹, H. Zohm¹ and the ASDEX Upgrade Team²

¹ *Max-Planck Institut für Plasmaphysik, 85748 Garching bei München, Germany*

² *See the author list of U. Stroth et al, Nucl. Fusion 62, 042006 (2022)*

Introduction

To prevent the occurrence of undesired events, like a disruption, a correct prediction of the plasma evolution of a tokamak discharge before it is actually performed is crucial. For this type of simulations, the models have to be fast and as much as possible based on first principles. A predictive tool who meets these requirements is a tokamak flight simulator [1]. This is a numerical tool which predicts the plasma behavior using the discharge program editor as input. It can ensure that either actuator trajectories or plasma parameters satisfy the experimental goals and reduces the probability of plasma disruptions and of exceeding operational limits. It is based on the interaction between control system, plasma equilibrium and transport.

Here a set of 4 physics models is developed for the transport description. Two models are applied in the confined region, depending on the regime of the plasma, while other two act in the Scrape-off-layer (SOL). They are linked through the last closed flux surface (LCFS). The simulations are run using ASTRA [2].

Core model

For the core turbulent transport a model based on analytical formulae fitted over a TGLF [3] database is used. Some threshold formulae have been adopted for ion temperature gradient (ITG), electron temperature gradient (ETG) and trapped electron mode (TEM), while Micro-Tearing-Modes (MTMs) have been neglected. The database consists of some stationary phases of 15 AUG discharges from different scenarios (H-mode, L-mode, I-mode and negative triangularity). Overall coordinates in the range $\rho_t = [0 - 1]$ have been considered. The formulae used for the fitting are reported here, in Gyrobohm units, that is $T_e^{1.5} B^{-2} a^{-1}$, where a is the minor radius of the LCFS:

$$\hat{\chi}_{i,ITG} = C \cdot H_{ITG} \left(\frac{R}{L_{Ti}} - \frac{R}{L_{Ti,ITG}} \right)^{\epsilon_{10}} q^{\gamma_q} e^{-\gamma_{\beta_e} \beta_e} k^{-\gamma_k} e^{-\gamma_{imp}(1-c_I)},$$

$$\hat{\chi}_{e,ETG} = D \cdot H_{ETG} \left(\frac{R}{L_{Te}} - \frac{R}{L_{Te,ETG}} \right)^{\epsilon_{20}} q^{\gamma_{q,e}} k^{-\gamma_{k,e}},$$

$$\hat{\chi}_{e,TEM} = D_2 H_{TEM} \left(\frac{R}{L_{Te}} - \frac{R}{L_{Te,TEM}} \right)^{\epsilon_{30}} e^{-\gamma_v v} e^{-\gamma_s s} e^{\gamma_{\delta,e} \delta}, \quad \hat{\chi}_{e,ITG} = \max \left\{ 1, f_t D_3 \frac{L_{Te}}{L_{Ti}} \right\} \hat{\chi}_{i,ITG},$$

H is a heaviside function, whose argument is the difference between the normalized temperature gradient and its threshold value. The linear threshold formulae are available from the literature

[4], [5]. From the TGLF simulations it has been noticed that over 95% of the transport is related to long-mixed scale turbulence. Thus through a disentanglement procedure ETG formula has been fitted on a small-scale-derived database. In figure 1 is shown the scattering of the TGLF coefficients compared to the respective values calculated by the fitting formulae. The particle

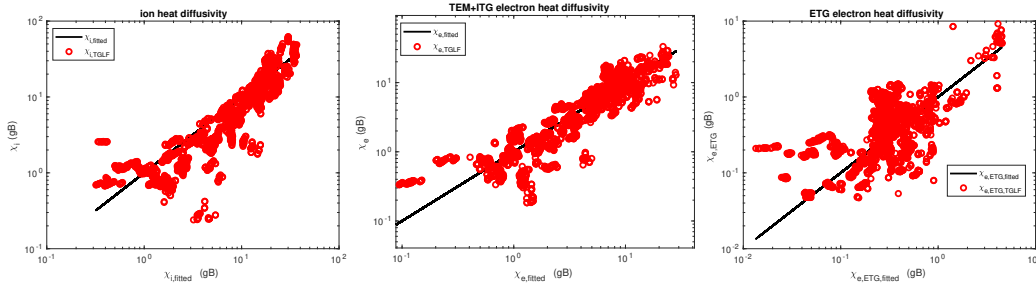


Figure 1: In red the transport coefficients calculated by TGLF vs the ones calculated by the fitting model, while in black is χ_{fitted} vs χ_{fitted} . On the left is shown ion heat diffusivity, while on the left TEM+ITG electron heat diffusivity. The lower plot is ETG electron heat diffusivity. The coefficients are shown in logarithmic scale.

diffusivity has been assumed to be equal to $C \cdot \chi_e$, where C is a calibration factor which has been fixed equal to 1 to match an experiment, while particle pinch has been modeled with a heuristic formula which is proportional to diffusivity to assure stationarity and takes into account the effect of L_{Te} , s and v . The convection is forced to be negative, that is a pinch, in order to have stationarity through the balance between particle diffusivity and particle pinch. This is not a limiting assumption for the majority of AUG discharge, which do not exhibit hollow density profiles.

Edge model

It is known that in the pedestal of high confinement mode (H-mode) the dynamic is usually mainly dominated by Edge Localized Modes (ELMs), while micro-turbulence is suppressed by sheared flows (as ExB shear). In this configuration an ELM average model has been adopted and the diffusivities have been assumed to lay on the marginal stability limit of the MHD peeling-ballooning model. In fact the temporal scale of these instabilities is much shorter than the duration of the discharge, so one can assume an average behaviour without leading to big limitations of the model when it is used within a flight simulator. By assuming a marginal stability on the MHD Peeling-Ballooning boundary a heuristic formula has been derived, which is based on a power law of the ratio between $\beta_{p,top}$ at the top of pedestal and $\beta_{p,MHD}$, which is the critical

value for the onset of the instability

$$\chi_e = \left(\frac{\beta_{p,top}}{\beta_{p,MHD}} \right)^4. \quad (1)$$

The critical value of β_p is calculated with a formula derived by a scaling on EPED [6] database, derived in [7]. The pedestal width in the normalized poloidal flux label has been fixed to 0.1. $\chi_i = \chi_e + \chi_{i,nc}$ has been assumed in this case. The particle diffusivity has been fixed to be equal to $C \cdot \chi_e$, where C has been fixed to 0.03 to match experimental stationary profiles in some discharges.

In L-mode the fitting model used for core has been extended to this region, while particle diffusivity was kept equal to $F \cdot \chi_e$, where F is calibrated to match experiments of the database ($F = 0.1$).

In order to predict the transition between L- and H-mode a criteria based on the ion power crossing the separatrix has been chosen, according to the Schmidtmayr scaling [8].

SOL models

To calculate the electron temperature at the separatrix a simple formula derived in [9] has been used, while the density is obtained by a particle balance in the SOL, which has been splitted in 6 different zones which confine with each other. This balance includes diffusive terms, ionizations and sources of plasma coming from the LCFS. Gas puff and vacuum pump are also included as source and sink. Some coefficients have been added in the equations to keep concentration gradients between confining regions unbalanced, in order to mimic convection. These are called enrichment factors and they multiply the density of species:

$$\frac{\partial N_k}{\partial t} = S + P + \sum_{j=1, j \neq k}^6 D_{jk} \left(\varepsilon_{jk} \frac{N_j}{V_j} - \frac{N_k}{V_k} \right) \quad (2)$$

In the previous equation S represents the source term, P is the sink, D_{jk} is the diffusion coefficient between the regions j and k , N is the number of particles, V is the volume and ε is the enrichment factor.

Results

A first fully integrated simulation of a H-mode discharge (40446) of ASDEX Upgrade in Fenix tokamak flight simulator has been run. One can see in figure 2 that the time trace of experimental β_p has been matched for the flattop and ramp-down phases. Also electron density and electron and ion temperature profiles have been matched along the discharge. A broader validation on multiple discharges including ramp-up is planned for the future.

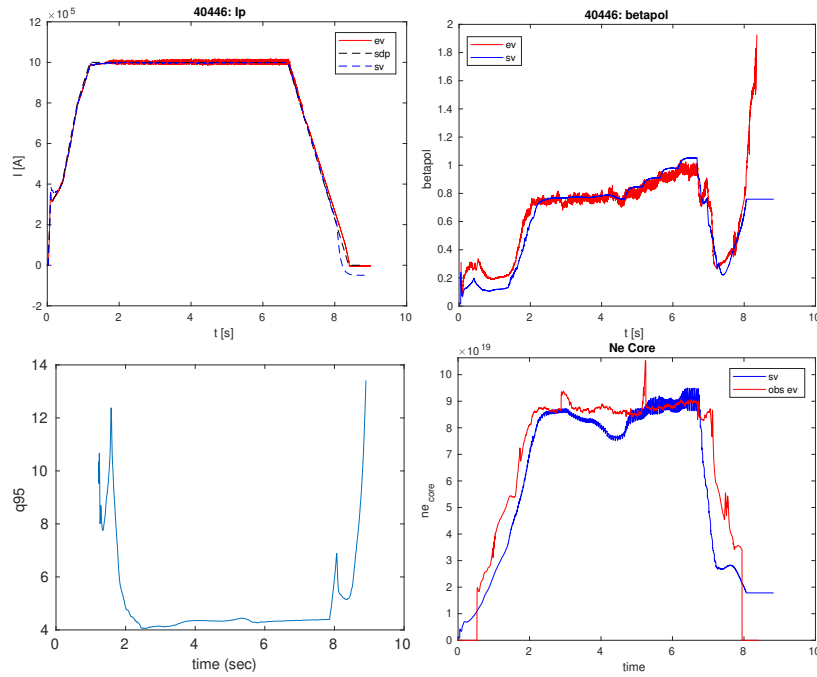


Figure 2: Clockwise time traces of I_p , β_p , $n_{e,avg}$ and q_{95} of a Fenix simulation of the discharge 40446 are shown. In red is the experimental trajectory and in blue the simulation.

Acknowledgments

This work has been carried out within the framework of the EUROfusion Consortium, funded by the European Union via the Euratom Research and Training Programme (Grant Agreement No 101052200 — EUROfusion). Views and opinions expressed are however those of the author(s) only and do not necessarily reflect those of the European Union or the European Commission. Neither the European Union nor the European Commission can be held responsible for them.

References

- [1] E. Fable et al., Plasma Phys. Control. Fusion 64 044002 (2022)
- [2] E. Fable et al., Plasma Physics and Controlled Fusion 55, 124028 (2013)
- [3] G.M. Staebler et al., Nucl. Fusion 57 066046 (2017)
- [4] F. Jenko et al., Physics of Plasmas 8, 4096 (2001)
- [5] A. G. Peeters et al., Phys. Plasmas 12, 022505 (2005)
- [6] P. B. Snyder et al. ,Phys. Plasmas 16, 056118 (2009)
- [7] J. Puchmayr, Optimization of Pedestal Stability on ASDEX Upgrade, IPP report 2020-11
- [8] Schmidtmayr M et al, Nucl. Fusion 58 056003 (2018)
- [9] R J Goldston et al., Plasma Phys. Control. Fusion 59 055015 (2017)